CARBON letters

Original Articles
Carbon Letters Vol. 28, 60-65 (2018)

Electronic transport properties of linear carbon chains encapsulated inside single-walled carbon nanotubes

Tomohiro Tojo[1,♠], Cheon Soo Kang[2], Takuya Hayashi[2], and Yoong Ahm Kim[3,4,♠]

[1]Department of Electrical and Electronic Information Engineering, Toyohashi University of Technology, Toyohashi 441-8580, Japan
[2]Faculty of Engineering, Shinshu University, Nagano 380-0928, Japan
[3]Department of Polymer Engineering, Graduate School, School of Polymer Science and Engineering & Alan G. MacDiarmid Energy Research Institute, Chonnam National University, Gwangju 61186, Korea
[4]Institute for Biomedical Sciences, Interdisciplinary Cluster for Cutting Edge Research, Shinshu University, Matsumoto 390-8621, Japan

Article Info
Received 30 January 2018
Accepted 9 March 2018

♠Corresponding Author
E-mail: tojo@ee.tut.ac.jp
yak@jnu.ac.kr
Tel: +81-538-45-0111

Open Access
DOI: http://dx.doi.org/10.5714/CL.2018.28.060

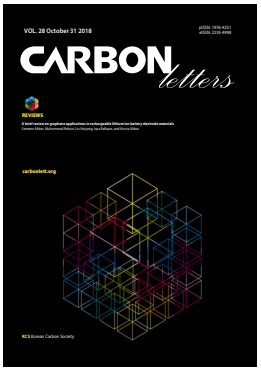

http://carbonlett.org

pISSN: 1976-4251
eISSN: 2233-4998

Abstract

Linear carbon chains (LCCs) encapsulated inside the hollow cores of carbon nanotubes (CNTs) have been experimentally synthesized and structurally characterized by Raman spectroscopy and transmission electron microscopy. However, in terms of electronic conductivity, their transportation mechanism has not been investigated theoretically or experimentally. In this study, the density of states and quantum conductance spectra were simulated through density functional theory combined with the non-equilibrium Green function method. The encapsulated LCCs inside (5,5), (6,4), and (9,0) single-walled carbon nanotubes (SWCNTs) exhibited a drastic change from metallic to semiconducting or from semiconducting to metallic due to the strong charge transfer between them. On the other hand, the electronic change in the conductance value of LCCs encapsulated inside the (7,4) SWCNT were in good agreement with the superposition of the individual SWCNTs and the isolated LCCs owing to the weak charge transfer.

Key words: linear carbon chains, single-walled carbon nanotubes, quantum conductance, non-equilibrium Green function method

1. Introduction

One-dimensional linear carbon chains (LCCs) have been anticipated to exhibit high tensile stiffness [1,2], controllable electronic band gaps [3,4], and high electron transport properties [1,5] when compared to any other known materials, thereby making them promising as next-generation electronic and optical devices [1-5]. LCCs consisting of *sp*-hybridized carbon atoms (known as carbynes) have two different configurations: (1) polyynes with alternating triple and single bonds and (2) cumulenes with consecutive double bonds [6]. Experimentally, such carbon chains have been synthesized using a variety of methods, such as carbon cluster beam deposition [7], laser ablation in an organic solution [8], chemical coupling [9], atomic peeling from graphene/carbon nanotubes (CNTs) [10,11], and encapsulation inside the cavity of single-walled (SW), double-walled (DW), and multi-walled (MW) CNTs [12-15]. Among them, the encapsulation method has increasingly been employed to stabilize LCCs inside the innermost confined spaces of their CNTs. Thus, being in such a confined nanosized space may prevent chemicals from interacting with LCCs because isolated LCCs have high reactivity of unsaturated *sp* hybridization orbitals against moisture or oxygen [16-18]. A detailed study of the electrical conductivity and reactivity of isolated LCCs using transmission electron microscopy (TEM) revealed the resistance change of the LCCs and their transformation from *sp* hybridization to other bonding forms due to joule heating and electron beam irradiation [19]. Therefore, CNTs are especially useful to stabilize the linear

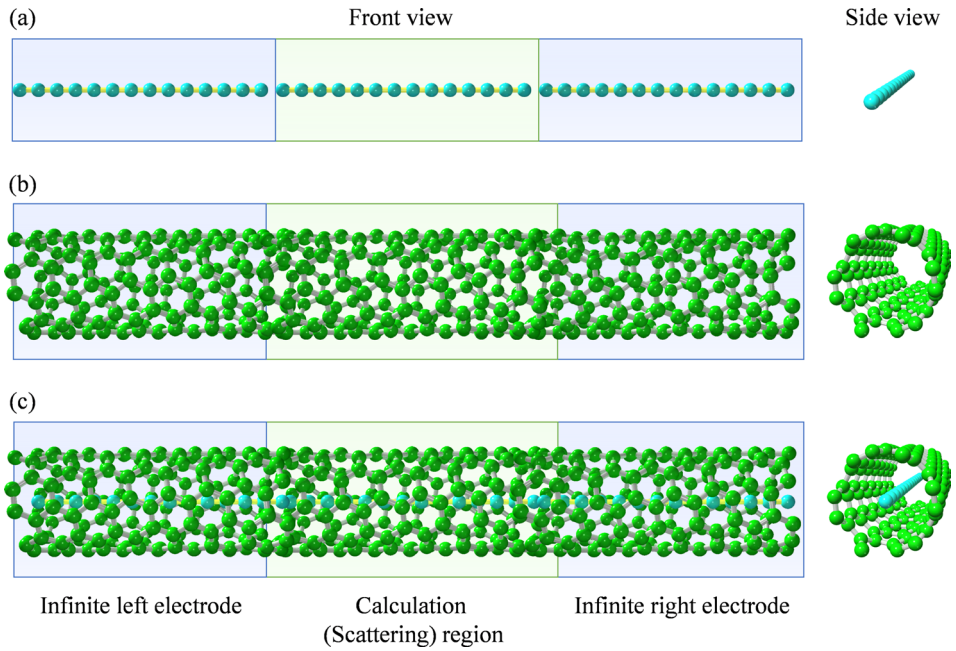

Fig. 1. Simulation models for electro-transportation on (a) isolated LCCs, (b) individual SWCNTs, and (c) LCCs-encapsulated SWCNTs.

structures of LCCs through van der Waals interaction with the innermost nanotubes.

The van der Waals interaction and charge transfer inside a nanotube, characterized by its chirality, strongly affect encapsulated LCCs, which are available in a variety of lengths and with various electronic features, such as metallic or semiconducting properties [12-15]. Experimentally, Raman spectroscopy is one of the most effective tools to investigate the interaction between CNT and the encapsulated LCCs. For example, the Raman active peak for encapsulated LCCs has been widely observed between 1800 and 2100 cm^{-1} [12-15] owing to the strong interaction between the charge transfer from the CNTs and the encapsulated LCCs depending on the chirality of the CNTs and the chain lengths of the LCCs [20,21]. However, there has been no experimental study of electro-transportation characteristics, such as charge transfer on encapsulated LCCs, until a recent study conducted the first evaluations of their electrical conductivity [20]. Theoretically, there is also a lack of an electro-transportation mechanism acting on the encapsulated LCCs inside the innermost nanotubes with an optimal diameter experimentally estimated to be approximately 0.7 nm [14].

In this work, we performed first-principles calculations to understand the electronic properties (i.e., quantum conductance) of LCCs encapsulated inside SWCNTs with diameters of around 0.7 nm. The SWCNTs were the (5,5), (6,4), (9,0), and (7,4) chirality types. Our theoretical results will be very meaningful to those involved in the fabrication of next-generation electronic devices.

2. Computational Details

In this work, we utilized density functional theory [22,23] combined with the non-equilibrium Green function method [24,25] and the Landauer formula [26] for electro-transportation of LCC-encapsulated SWCNTs under a periodic boundary condition in all directions (i.e., the *x, y, z* axes). As shown in Fig. 1, the simulation models consisted of three regions, that is, a central scattering region and two semi-infinite left/right electrodes represented by a supercell with repeated unit cells. The C-C bond distances for the isolated polyyne were set alternately at $d_{\text{poly-single}}$ = 1.51Å and $d_{\text{poly-triple}}$ = 1.22Å, while that for the cumulene was consecutively $d_{\text{cumu-double}}$ = 1.37Å [27]. Using a bond distance of 1.421Å in graphite [28], the SWCNTs were modeled with (5,5), (6,4), (9,0), and (7,4) chirality, with estimated diameters of 6.785, 6.830, 7.051, and 7.555 Å, respectively. After electronic calculations of the LCC-encapsulated SWCNTs, the unit cells were chosen such that good agreement within 0.5% tolerance in length was ensured between the encapsulated LCCs and SWCNTs. A rectangular supercell of *a* [Å]×25 Å×25 Å (where *a* is the lengthwise axis of the unit cell) was used.

All calculations for quantum conductance on the models were carried out using the Open source package for Material eXplorer (OpenMX, ver. 3.6 code [29]) within the local density approximation (LDA) [30] for the exchange-correlation functionals and norm-conserving pseudopotentials [31]. In this study, we chose the LDA because it provides a bound state of carbon-based materials with a lattice parameter of 2.46 Å in graphite [32]. A cut-off energy of 200 Ry was chosen with the energy convergence criterion of 10^{-10} Hartree, and the vacuum layers were set to ~20 Å in the periodic directions (with the exception of the *a* axis to prevent electronic interactions between adjacent cells). In addition, 200×1×1 *k*-point grids were used for all models. The electronic temperature was set to 27˚C for the counting of the electron number.

3. Results and Discussion

Fig. 2 shows the density of states (DOS) and quantum conductance values represented by $G_0 = 2e^2/h = 1/12.9$ mS [33] for an isolated polyyne and cumulene. As clearly indicated in Fig. 2a, the isolated polyyne has a wide band gap of E_g=2.51 eV, indicating a semiconducting property corresponding to the conductance of $0G_0$ at the Fermi level (E_F) in Fig. 2b. On the other hand, the Fermi level for the cumulene was located in the conduction band (Fig. 2c), indicating a metallic property corresponding to the conductance of $2G_0$ in Fig. 2d. These features of both the polyyne and cumulene are in good agreement with other theoretical calculations [27].

The DOS for an individual (5,5) SWCNT showed the metallic property with van Hove singularities at the higher sub-bands (Fig. 3a), thereby displaying high conductance of $2G_0$ (Fig. 3b) as two sub-bands cross the Fermi level [34]. Conversely, Fig. 3c shows that the DOS for an individual (6,4) SWCNT was a semiconductor with a band gap of E_g=1.06 eV, which is consistent with earlier experimental and theoretical studies [35]. Therefore, its semiconducting property led to low conductance of $0G_0$ (Fig. 3d). While it is known that zigzag (9,0) and (7,4) SWCNTs with a narrow diameter are small-gap semiconductors [36], they are generally expected to have metallic properties corresponding to armchair (*n*,*n*) SWCNTs due to a curvature effect [36]; the corresponding DOS spectra in the inset images of Fig. 3e and g show a small gap near the Fermi level. On the other hand, these quantum conductance values in Fig. 3f and h present metallic values of approximately $2G_0$ at the Fermi level. When focusing on these conductances around the Fermi level, a sharp peak was observed in each of the (9,0) and (7,4) SWCNTs, suggesting strong hybridization of *sp* orbitals in nanotubes with narrow diameters [36,37].

The DOS and conductance spectra for the LCCs inside the SWCNTs are depicted in Figs. 4 and 5. Interestingly, two new peaks appeared near the Fermi level in the DOS spectra for the polyyne-encapsulated (5,5) SWCNT (Fig. 4a), leading to an increment in the conductance from $2G_0$ for an individual (5,5) SWCNT to $3G_0$ (Fig. 4b), despite the fact that an isolated polyyne is a semiconducting property. Comparing the DOS spectra for cumulene-encapsulated (5,5) SWCNT (Fig. 5a) with that of the individual (5,5) SWCNT, there was no dramatic change in the shape of the DOS spectra even considering that the conductance was $0G_0$ (Fig. 5b), corresponding to a semiconducting property. Therefore, electronic changes in conductances are thought to be due to charge transfer and hybridization effects between SWCNTs and LCCs [38]. In fact, the charge transfer values were calculated to be 0.05 and >0.05 electrons per atom on polyyne and cumulene inside the (5,5) SWCNT, respectively. This suggests strong interactions of LCCs inside SWCNTs with an interactive narrow space. The enhancement and reduction caused by the charge transfer could be seen in the DOS and conductance spectra for the polyyne-/cumulene-encapsulated (6,4) SWCNT and the (9,0) SWCNT (Figs. 4 and 5c-f). At the same time, the conductance values for the

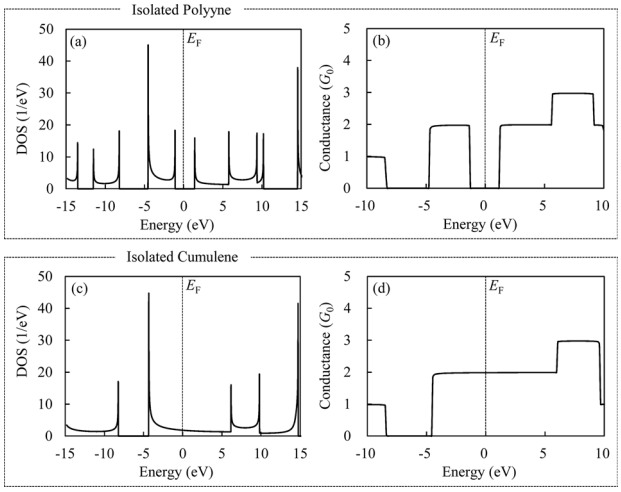

Fig. 2. Density of states (DOS) and quantum conductance for an isolated (a, b) polyyne and (c, d) cumulene.

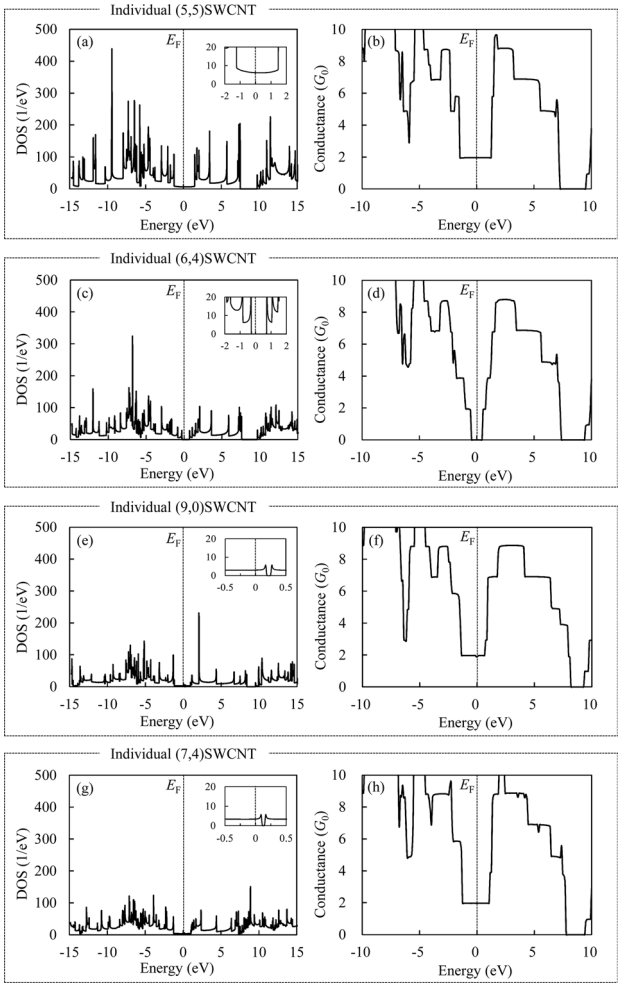

Fig. 3. Density of states (DOS) and quantum conductance for an individual (a, b) (5,5) SWCNT, (c, d) (6,4) SWCNT, (e, f) (9,0) SWCNT, and (g, h) (7,4) SWCNT. Here, E_F with the dotted line denotes the Fermi level. Inset images in the DOS spectra present enlarged views near the Fermi level.

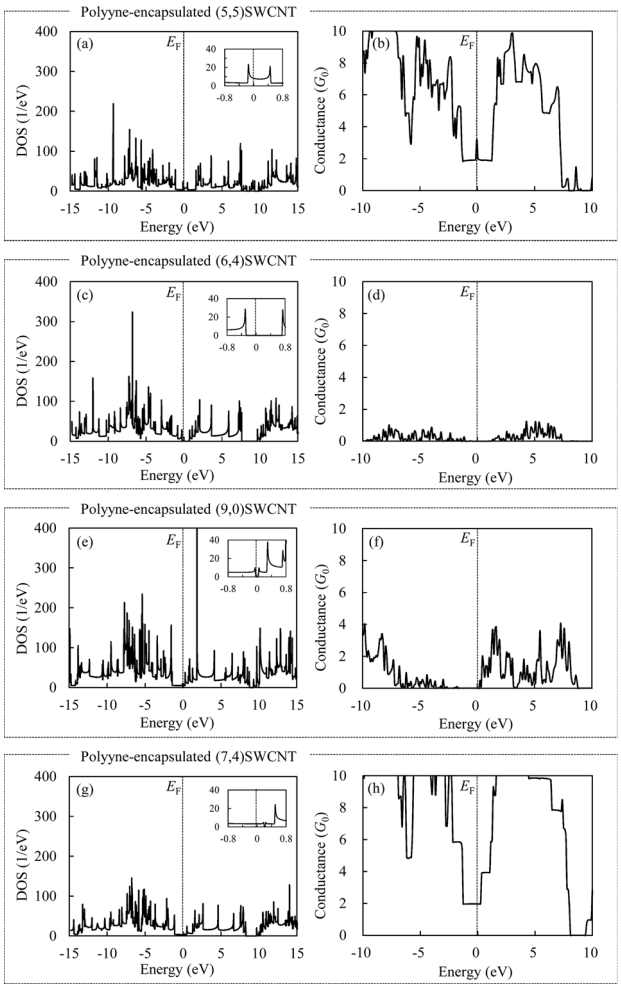

Fig. 4. Density of states (DOS) and quantum conductance for a polyyne-encapsulated (a, b) (5,5) SWCNT, (c, d) (6,4) SWCNT, (e, f) (9,0) SWCNT, and (g, h) (7,4) SWCNT. E_F with the dotted line indicates the Fermi level. Inset images in the DOS spectra present enlarged views near the Fermi level.

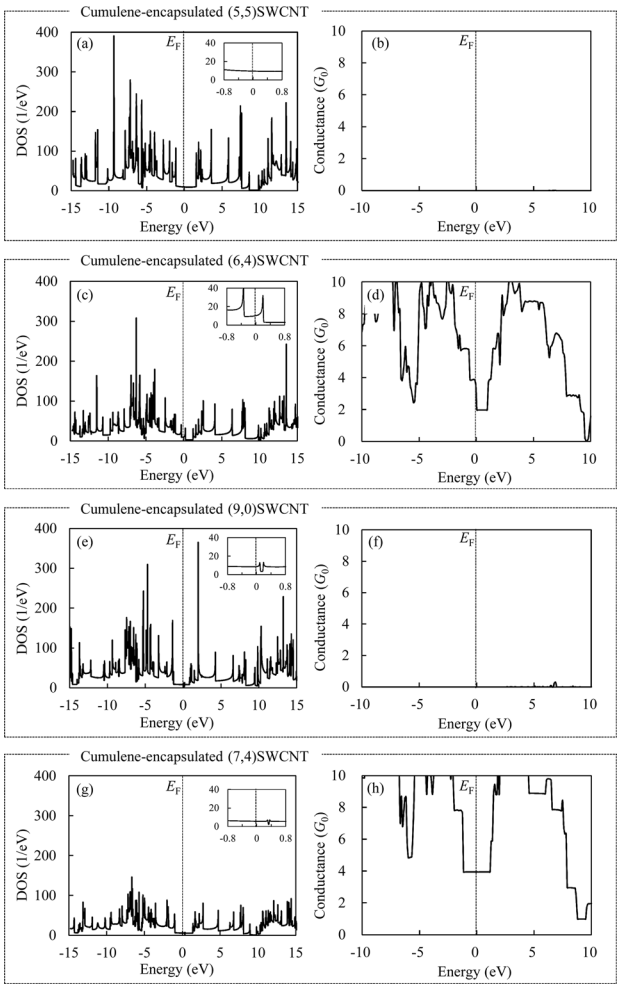

Fig. 5. Density of states (DOS) and quantum conductance for a cumulene-encapsulated (a, b) (5,5) SWCNT, (c, d) (6,4) SWCNT, (e, f) (9,0) SWCNT, and (g, h) (7,4) SWCNT. E_F with the dotted line represents the Fermi level. Inset images in the DOS spectra present enlarged views near the Fermi level.

polyyne-/cumulene-encapsulated (7,4) SWCNT (Figs. 4, 5g and h), which are estimated to be $2G_0$ and $4G_0$ respectively, are in good agreement with the superposition of that of an individual (7,4) SWCNT and an isolated polyyne/cumulene despite the fact that the DOS spectra possess a new peak near the Fermi level, as shown in Fig. 4g. Therefore, it can be concluded that there is low significant charge transfer (0.01–0.03 electrons per atom) between the LCCs and the (7,4) SWCNT due to the larger diameter than that of the other samples. These results, taken together, suggest that the electronic behaviors of the (5,5), (6,4), and (9,0) SWCNTs are easily controllable compared to those of the (7,4) SWCNT due to their strong interactions.

4. Conclusions

In this study, we performed first-principles simulations of the DOS and quantum conductance on LCCs encapsulated inside SWCNTs in order to determine the encapsulation effect on the electronic behaviors. The quantum conductance values varied from metallic to semiconducting or from semiconducting to metallic with differences in the diameters of the (5,5), (6,4), and (9,0) SWCNTs owing to the strong interaction (*i.e.,* charge transfer and hybridization effects). For the (7,4) SWCNT with the larger diameter, the conductance values varied with the superposition of that of the individual tube and an isolated LCC. Therefore, LCCs encapsulation into smaller tubes would have a stronger influence on the electronic behaviors than those encapsulated into larger tubes.

Conflict of Interest

No potential conflict of interest relevant to this article was reported.

Acknowledgements

T.T. acknowledges the support from the Grant-in-Aid for Toyota Physical and Chemical Research Institute Scholar Project and from the Naito Science & Engineering Foundation. Y.A.K. acknowledges the financial support in the form of a grant from the National Research Foundation of Korea (NRF) funded by the Korean government (MSIP) (No. NRF-2017R1A2A1A17069771) and from the Nano Material Technology Development Program through the NRF funded by the Ministry of Science, ICT and Future Planning (2016M3A7B4021149).

References

[1] Liu M, Artyukhov VI, Lee H, Xu F, Yakobson BI. Carbyne from first principles: chain of C atoms, a nanorod or a nanorope. ACS Nano, **7**, 10075 (2013). https://doi.org/10.1021/nn404177r.

[2] Timoshevskii A, Kotrechko S, Matviychuk Y. Atomic structure and mechanical properties of carbyne. Phys Rev B, **91**, 245434 (2015). https://doi.org/10.1103/physrevb.91.245434.

[3] Weimer M, Hieringer W, Sala FD, Görling A. Electronic and optical properties of functionalized carbon chains with the localized Hartree–Fock and conventional Kohn–Sham methods. Chem Phys, **309**, 77 (2005). https://doi.org/10.1016/j.chemphys.2004.05.026.

[4] Ming C, Meng FX, Chen X, Zhuang J, Ning XJ. Tuning the electronic and optical properties of monatomic carbon chains. Carbon, **68**, 487 (2014). https://doi.org/10.1016/j.carbon.2013.11.025.

[5] Kotrechko S, Timoshevskii A, Kolyvoshko E, Matviychuk Y, Stetsenko N. Thermomechanical stability of carbyne-based nanodevices. Nanoscale Res Lett, **12**, 327 (2017). https://doi.org/10.1186/s11671-017-2099-4.

[6] Alkorta I, Elguero J. Polyynes vs. cumulenes: their possible use as molecular wires. Struct Chem, **16**, 77 (2005). https://doi.org/10.1007/s11224-005-1089-9.

[7] Casari CS, Bassi AL, Ravagnan L, Siviero F, Lenardi C, Piseri P, Bongiorno G, Bottani CE, Milani P. Chemical and thermal stability of carbyne-like structures in cluster-assembled carbon films. Phys Rev B, **69**, 075422 (2004). https://doi.org/10.1103/physrevb.69.075422.

[8] Tsuji M, Tsuji T, Kuboyama S, Yoon SH, Korai Y, Tsujimoto T, Kubo K, Mori A, Mochida I. Formation of hydrogen-capped polyynes by laser ablation of graphite particles suspended in solution. Chem Phys Lett, **355**, 101 (2002). https://doi.org/10.1016/s0009-2614(02)00192-6.

[9] Chalifoux WA, Tykwinski RR. Synthesis of polyynes to model the sp-carbon allotrope carbyne. Nat Chem, **2**, 967 (2010). https://doi.org/10.1038/nchem.828.

[10] Jin C, Lan H, Peng L, Suenaga K, Iijima S. Deriving carbon atomic chains from graphene. Phys Rev Lett, **102**, 205501 (2009). https://doi.org/10.1103/physrevlett.102.205501.

[11] Rinzler AG, Hafner JH, Nikolaev P, Nordlander P, Colbert DT, Smalley RE, Lou L, Kim SG, Tománek D. Unraveling nanotubes: field emission from an atomic wire. Science, **269**, 1550 (1995). https://doi.org/10.1126/science.269.5230.1550.

[12] Nishide D, Dohi H, Wakabayashi T, Nishibori E, Aoyagi S, Ishida M, Kikuchi S, Kitaura R, Sugai T, Sakata M, et al. Single-wall carbon nanotubes encaging linear chain $C_{10}H_2$ polyyne molecules inside. Chem Phys Lett, **428**, 356 (2006). https://doi.org/10.1016/j.cplett.2006.07.016.

[13] Zhao C, Kitaura R, Hara H, Irle S, Shinohara H. Growth of linear carbon chains inside thin double-wall carbon nanotubes. J Phys Chem C, **115**, 13166 (2011). https://doi.org/10.1021/jp201647m.

[14] Zhao X, Ando Y, Liu Y, Jinno M, Suzuki T. carbon nanowire made of a long linear carbon chain inserted inside a multiwalled carbon nanotube. Phys Rev Lett, **90**, 187401 (2003). https://doi.org/10.1103/physrevlett.90.187401.

[15] Shi L, Rohringer P, Suenaga K, Niimi Y, Kotakoski J, Meyer JC, Peterlik H, Wanko M, Cahangirov S, Rubio A, et al. Confined linear carbon chains as a route to bulk carbyne. Nat Mater, **15**, 634 (2016). https://doi.org/10.1038/nmat4617.

[16] Muramatsu H, Hayashi T, Kim YA, Shimamoto D, Endo M, Terrones M, Dresselhaus MS. Synthesis and isolation of molybdenum atomic wires. Nano Lett, **8**, 237 (2008). https://doi.org/10.1021/nl0725188.

[17] Kitaura R, Nakanishi R, Saito T, Yoshikawa H, Awaga K, Shinohara H. High-yield synthesis of ultrathin metal nanowires in carbon nanotubes. Angew Chem Int Ed, **48**, 8298 (2009). https://doi.org/10.1002/anie.200902615.

[18] Lagow RJ, Kampa JJ, Wei HC, Battle SL, Genge JW, Laude DA, Harper CJ, Bau R, Stevens RC, Haw JF, et al. Synthesis of linear acetylenic carbon: the "sp" carbon allotrope. Science, **267**, 362 (1995). https://doi.org/10.1126/science.267.5196.362.

[19] Romdhane FB, Adjizian JJ, Charlier JC, Banhart F. Electrical transport through atomic carbon chains: the role of contacts. Carbon, **122**, 92 (2017). https://doi.org/10.1016/j.carbon.2017.06.039.

[20] Kang CS, Fujisawa K, Ko YI, Muramatsu H, Hayashi T, Endo M, Kim HJ, Lim D, Kim JH, Jung YC, et al. Linear carbon chains inside multi-walled carbon nanotubes: growth mechanism, thermal stability and electrical properties. Carbon, **107**, 217 (2016). https://doi.org/10.1016/j.carbon.2016.05.069.

[21] Wanko M, Cahangirov S, Shi L, Rohringer P, Lapin ZJ, Novotny L, Ayala P, Pichler T, Rubio A. Polyyne electronic and vibrational properties under environmental interactions. Phys Rev B, **94**, 195422 (2016). https://doi.org/10.1103/physrevb.94.195422.

[22] Hohenberg P, Kohn W. Inhomogeneous electron gas. Phys Rev, **136**, B864 (1964). https://doi.org/10.1103/physrev.136.b864.

[23] Kohn W, Sham LJ. Self-consistent equations including exchange and correlation effects. Phys Rev, **140**, A1133 (1965). https://doi.org/10.1103/physrev.140.a1133.

[24] Datta S. Electronic Transport in Mesoscopic Systems, Cambridge University Press, New York, 293 (1995).

[25] Ozaki T, Nishio K, Kino H. Efficient implementation of the nonequilibrium Green function method for electronic transport calculations. Phys Rev B, **81**, 035116 (2010). https://doi.org/10.1103/physrevb.81.035116.

[26] Landauer R. Spatial variation of currents and fields due to localized scatterers in metallic conduction. IBM J Res Dev, **1**, 223 (1957). https://doi.org/10.1147/rd.13.0223.

[27] Calzolari A, Marzari N, Souza I, Nardelli MB. Ab initiotransport properties of nanostructures from maximally localized Wannier functions. Phys Rev B, **69**, 035108 (2004). https://doi.org/10.1103/physrevb.69.035108.

[28] Dresselhaus MS, Dresselhaus G, Saito R, Jorio A. Raman spectroscopy of carbon nanotubes. Phys Rep, **409**, 47 (2005). https://doi.org/10.1016/j.physrep.2004.10.006.

[29] OpenMX ver. 3.6, Ozaki T group in the University of Tokyo, 2000. Available from: http://www.openmx-square.org.

[30] Ceperley DM, Alder BJ. Ground state of the electron gas by a stochastic method. Phys Rev Lett, **45**, 566 (1980). https://doi.org/10.1103/physrevlett.45.566.

[31] Troullier N, Martine JL. Efficient pseudopotentials for plane-wave calculations. Phys Rev B, **43**, 1993 (1991). https://doi.org/10.1103/physrevb.43.1993.

[32] Woods LM, Bădescu SC, Reinecke TL. Adsorption of simple benzene derivatives on carbon nanotubes. Phys Rev B, **75**, 155415 (2007). https://doi.org/10.1103/physrevb.75.155415.

[33] Frank S, Poncharal P, Wang ZL, de Heer WA. Carbon nanotube quantum resistors. Science, **280**, 1744 (1998). https://doi.org/10.1126/science.280.5370.1744.

[34] Kienle D, Cerda JI, Ghosh AW. Extended Hückel theory for band structure, chemistry, and transport. I. Carbon nanotubes. J Appl Phys, **100**, 043714 (2006). https://doi.org/10.1063/1.2259818.

[35] Wei X, Tanaka T, Yomogida Y, Sato N, Saito R, Kataura H. Experimental determination of excitonic band structures of single-walled carbon nanotubes using circular dichroism spectra. Nat Commun, **7**, 12899 (2016). https://doi.org/10.1038/ncomms12899.

[36] Ouyang M, Huang JL, Cheung CL, Lieber CM. Energy gaps in "Metallic" single-walled carbon nanotubes. Science, **292**, 702 (2001). https://doi.org/10.1126/science.1058853.

[37] Blase X, Benedict LX, Shirley EL, Louie SG. Hybridization effects and metallicity in small radius carbon nanotubes. Phys Rev Lett, **72**, 1878 (1994). https://doi.org/10.1103/physrevlett.72.1878.

[38] Tapia A, Aguiler L, Cab C, Medina-Esquivel RA, de Coss R, Canto G. Density functional study of the metallization of a linear carbon chain inside single wall carbon nanotubes. Carbon, **48**, 4057 (2010). https://doi.org/10.1016/j.carbon.2010.07.011.